DOI: 10.1002/ejic.200600925

Resonance Raman Spectroscopy with Overtones Involving Metal-Ligand and Ligand-Centered Modes in (*o*-Benzoquinonediimine)ruthenium(II) Complexes

Rémi Beaulac,[a] A. B. P. Lever,*[b] and Christian Reber*[a]

Keywords: Raman spectroscopy / Ruthenium complexes / *o*-Benzoquinonediimine / Electronic structure / Covalency / π-Back donation / Charge transfer / Density functional calculations / Overtones / Combination bands / Luminescence / Absorption

Resonance Raman spectra of (*o*-benzoquinonediimine)ruthenium(II) complexes measured with visible excitation wavelengths show distinct resonance enhancements and intense overtone and combination bands. Assignments of the most prominent fundamental bands are made on the basis of comparisons with theoretical spectra obtained from DFT calculations. Excited state distortions are determined from the resonance Raman intensities and lead to calculated luminescence and absorption spectra in good agreement with experiment.

Introduction

Resonance Raman spectroscopy can be used as a powerful technique to study excited-state structure, in particular for systems with broad, unresolved absorption transitions that do not provide detailed information through resolved vibronic structure.[1–5] Charge-transfer processes in transition-metal complexes, in particular those of ruthenium(II), are of particular interest for spectroscopic investigations, as detailed spectra combined with theoretical models provide quantitative insight on the structural and dynamics aspects of these important excited states.[6,7] In the vast majority of reported resonance Raman studies on ruthenium(II) complexes only fundamental bands are observed.[7–10,11]

The ligand *o*-benzoquinonediimine (BQDI) and its derivatives are of interest because of the extensive delocalization of Ru 4d electron density over the BQDI ligand.[12–18] This delocalization has been discussed in terms of metal–ligand orbital mixing or donor–acceptor electronic coupling. The covalent interactions between the metal and the ligand can be separated into ligand-to-metal donation and metal-to-ligand back-donation.[12–18] Complexes with these ligands, in particular [Ru(BQDI)(acac)$_2$] and [Ru(BQDI)(NH$_3$)$_2$Cl$_2$], show resonance Raman spectra with exceptionally rich patterns involving harmonics and combination bands. We present and analyze these spectra in the following report.

Results and Discussion

Resonance Raman spectra of [Ru(BQDI)(acac)$_2$] and [Ru(BQDI)(NH$_3$)$_2$Cl$_2$] were measured with excitation wavelengths near the lowest-energy intense absorption maximum at ca. 20000 cm^{-1}, and are shown in Figure 1. Strong resonance enhancements are accompanied by an exceptionally detailed series of overtones and combination bands (identified by the labels I, II, III), which provide relevant information on excited-state distortions in the title complexes. Raman spectra measured with off-resonance excitation at 12700 cm^{-1} are compared to the resonance Raman spectra in Figure 2. It is likely that each peak observed in the off-resonance Raman spectra corresponds to a fundamental transition, as overtones and combination bands are too weak to be observed in the absence of resonance enhancements; we can identify on the order of 16–18 experimental vibrational frequencies as listed in Table 1. The comparison of resonance and off-resonance spectra shows very clearly

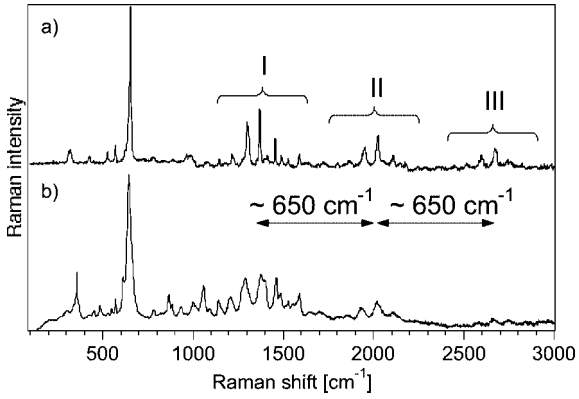

Figure 1. Comparison of resonance Raman spectra (solid samples, 77 K) of a) [Ru(BQDI)(NH$_3$)$_2$Cl$_2$] (λ_{exc} = 488 nm) and of b) [Ru(BQDI)(acac)$_2$] (λ_{exc} = 514 nm). The baseline was corrected to remove the luminescence onset and the total integrated intensity of each spectrum was normalized.

[a] Département de chimie, Université de Montréal, Montréal QC H3C 3J7, Canada
[b] Department of Chemistry, York University, CB124, 4700 Keele Street, Toronto, ON M3J 1P3, Canada

that all peaks observed at frequencies between 1700 cm^{-1} and 3000 cm^{-1} correspond to resonance-enhanced overtones or combination bands. Calculated Raman spectra obtained from DFT are in good agreement with the experimental spectra, as shown by the dotted traces in Figure 2. In particular, the calculated spectra do not show any bands where overtones and combination bands are observed, and they indicate a larger number of bands in the 1200 to 1500 cm^{-1} region for [Ru(BQDI)(acac)$_2$] than for [Ru(BQDI)(NH$_3$)$_2$Cl$_2$], providing a qualitative rationale for the large, poorly resolved feature observed for the former complex in this wavenumber range. The Raman peaks in the off-resonance spectrum of [Ru(BQDI)(acac)$_2$] are weak and broad, especially in the 1200 to 1500 cm^{-1} region, complicating the identification of fundamental bands. Only the peaks that can clearly be assigned as fundamentals involved in the resonance Raman spectrum were labeled as such in Figure 2 and in Table 1.

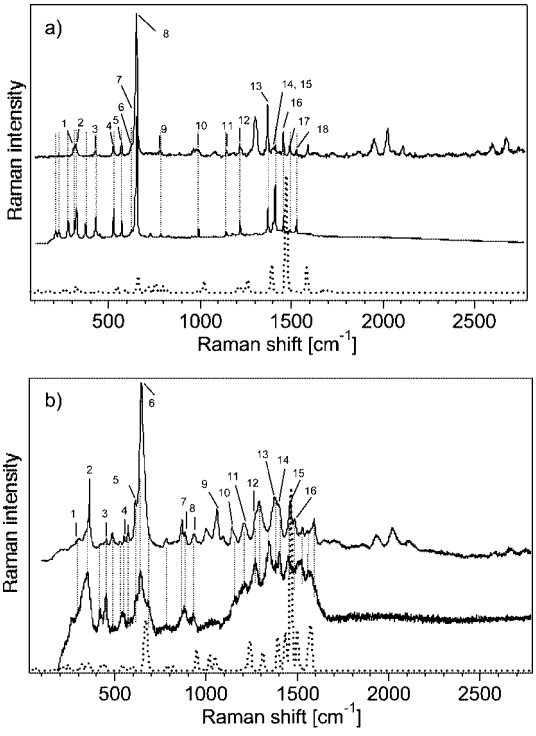

Figure 2. Comparison of resonance Raman (top spectrum) and off-resonance Raman (middle spectrum) in solid phase at 77 K and (lower) DFT calculated spectrum. a) [Ru(BQDI)(NH$_3$)$_2$Cl$_2$], top: λ_{exc} = 488 nm, middle: λ_{exc} = 788 nm. b) [Ru(BQDI)(acac)$_2$], top: λ_{exc} = 514 nm, middle: λ_{exc} = 788 nm. The number labels refer to Table 1.

All peaks observed in the resonance Raman spectra not corresponding to fundamental frequencies are assigned as harmonics or combination bands built on one or several of the fundamental frequencies listed in Table 1. The analysis of the Raman spectra of [Ru(BQDI)(NH$_3$)$_2$Cl$_2$] is more straightforward because the identification of the fundamental frequencies in the off-resonance Raman spectrum is obvious. In both systems, it appears clearly that the peaks labeled II and III in Figure 1 observed at Raman shifts of approximately 2000 cm^{-1} and 2600 cm^{-1} are not fundamentals, and their spacing of approximately 650 cm^{-1} corresponds to the Raman shift of the most intense peak in each resonance Raman spectrum, observed at 655 and 646 cm^{-1} in [Ru(BQDI)(NH$_3$)$_2$Cl$_2$] and [Ru(BQDI)(acac)$_2$], respectively. The high relative intensities of the transitions at 655 and 646 cm^{-1} show directly that the largest distortions between the ground-state and the excited-state structures probed here occur along the normal coordinates of these modes and that the peaks in regions II and III are combination bands involving these modes. The peaks in region I are not as easily identified, as both fundamental bands and the first overtone of the most intense fundamental occur at the Raman shifts of approximately 1300 cm^{-1} corresponding to this region and calculated spectra have to be used to identify individual transitions.

Table 1. Observed vibrational frequencies ω_k [cm^{-1}] and calculated excited-state distortions Δ_k [dimensionless] of the modes observed in the resonance Raman spectra of [Ru(BQDI)(NH$_3$)$_2$Cl$_2$] and [Ru(BQDI)(acac)$_2$]. The index k refers to the numerical labels shown in Figure 2 and numbers the normal coordinates in Equation (3); the parameters E_{00} and Γ refer to Equation (2).

	[Ru(BQDI)(NH$_3$)$_2$Cl$_2$]		[Ru(BQDI)(acac)$_2$]	
k	ω_k	Δ_k	ω_k	Δ_k
1	314	1.0	306	1.0
2	324	1.0	355	1.2
3	427	0.5	454	0.5
4	527	0.6	550	0.7
5	572	0.9	613	1.0
6	624	0.6	646	2.0
7	645	1.3	886	0.5
8	655	2.0	934	0.4
9	782	0.3	1058	0.6
10	992	0.3	1142	0.4
11	1145	0.2	1208	0.4
12	1218	0.3	1270	0.5
13	1370	0.8	1378	0.6
14	1398	0.2	1400	0.5
15	1413	0.2	1460	0.5
16	1456	0.5	1484	0.4
17	1491	0.2		
18	1528	0.2		
Total distortion $\sum_k \Delta_k$		11.1		11.2
E_{00} [cm^{-1}]		17250		16830
Γ [cm^{-1}]		150		400

The DFT calculations are used to assign the most prominent observed Raman transitions. Calculated at 665 cm^{-1} and 662 cm^{-1} are the Ru–NH(BQDI) stretching modes for [Ru(BQDI)(NH$_3$)$_2$Cl$_2$] and [Ru(BQDI)(acac)$_2$], respectively, which involve fairly large breathing motion in the BQDI ring for both complexes. These frequencies are higher by 10 and 16 cm^{-1} than the experimental values, illustrating the excellent quantitative agreement. The 1394 and 1392 cm^{-1} peaks correspond to the C=NH vibration coupled strongly to the CH bonds localized on the BQDI ligand. The calculated frequencies are higher than the experimental values by 24 and 14 cm^{-1} for [Ru(BQDI)(NH$_3$)$_2$Cl$_2$] and [Ru(BQDI)(acac)$_2$], respectively. The calculated vibrational frequencies tend to be slightly higher than the experimental values,

possibly due to the B3LYP functional slightly over-emphasizing the covalent contribution to the Ru–N bonds,[19] but overall the agreement between calculated and observed frequencies is excellent.

A quantitative analysis of the resonance Raman intensities leads to a more precise picture of excited-state distortions and allows us to identify similarities and differences between the two compounds studied here. The resonance Raman intensities can be calculated very efficiently using the time-dependent approach described previously by Heller, Zink and associates.[1,3,4,20–22] The simplest approach, used here, is based on a single electronic excited state and the Raman intensity $I_{i\rightarrow f}$ at frequency ω_s is given by Equation (1):

$$I_{i\rightarrow f} \propto \omega_I \omega_S{}^3 \left[\alpha_{fi}\right]^* \left[\alpha_{fi}\right] \quad (1)$$

with Equation (2):

$$\left[\alpha_{fi}\right] = \frac{i}{\hbar}\int_0^\infty \left\langle \phi_f \middle| \phi(t)\right\rangle \cdot exp\left(-iE_{00}t - \Gamma t\right) \cdot \exp\left(i\left(\omega_i + \omega_I\right)t\right)dt \quad (2)$$

where Γ is a constant damping factor (in cm^{-1}), $\hbar\omega_i$ is the zero-point energy of the ground electronic potential energy surface and $\hbar\omega_I$ is the energy of the incident radiation. $\langle\phi_f|\phi(t)\rangle$ is the autocorrelation function, which takes a simple analytical form if it is assumed that (a) the force constants are the same in both ground and excited states, (b) the potential energy surfaces are harmonic, (c) the transition dipole moment is independent of the normal coordinates and (d) the normal coordinates are not coupled, see Equation (3).

ω_k and Δ_k denote the wavenumber (in cm^{-1}) and the difference between potential-energy minima of the ground and excited states along the kth normal coordinate, respectively, and n_k is the vibrational quantum number of the kth normal mode in the ground electronic state. As an example, the combination band ($2\nu_1 + \nu_2$) in a three-mode case would have $n_1 = 2$, $n_2 = 1$ and $n_3 = 0$. Equation (1) can be used to calculate the excitation profile for each fundamental, harmonic and combination band involved in the resonance Raman spectrum. The experimental spectra in Figure 1 and Figure 2 do not provide full excitation profiles, but an analysis is still possible. The approach consists of adjusting the ratio of intensities between calculated profiles for different modes by fitting the displacements $\Delta_k{}^{n_k}$ in Equation (3) until the ratios of calculated intensities are in agreement with the experiment. Adjusting as many parameters as there are in Table 1 can be tedious, but the task is somewhat facilitated by using Savin's approximation to estimate the relative displacements between two modes k and k' in the resonance Raman spectrum [Equation (4)].[4]

$$\frac{I_k}{I_{k'}} = \left(\frac{\Delta_k \omega_k}{\Delta_{k'} \omega_{k'}}\right)^2 \quad (4)$$

The best parameter values obtained in this way are given in Table 1 for both complexes; the calculated intensities are compared to the experimental resonance Raman spectra in Figure 3 and Figure 4 for $[Ru(BQDI)(NH_3)_2Cl_2]$ and $[Ru(BQDI)(acac)_2]$, respectively. These calculations involve all modes identified as fundamentals in the experimental Raman spectra, in contrast to the simplified analysis for $[Ru(BQDI)(NH_3)_2Cl_2]$,[18] where only five modes were considered. Figure 3 and Figure 4 illustrate the very good agreement between calculated and experimental intensities of the resonance Raman spectra. An additional criterion to compare model calculations and experimental spectra is provided by the intensities of overtones and combination bands, which are also reproduced well, as shown for the first overtone of the 650 cm^{-1} mode in Figure 3 and Fig-

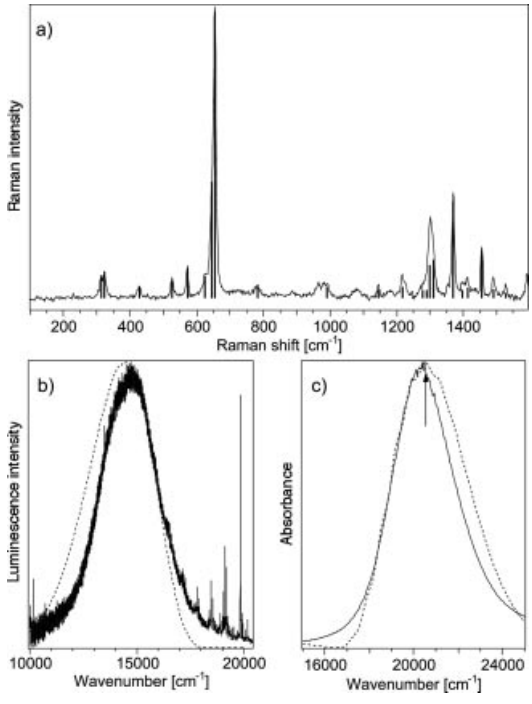

Figure 3. Comparison of calculated and experimental spectra for $[Ru(BQDI)(NH_3)_2Cl_2]$. a) Resonance Raman, b) 77 K solid-state luminescence and c) room-temperature absorption in dimethylformamide solution. The calculated spectra in b) and c) are given as dotted lines. The vertical arrow in c) indicates the resonance Raman excitation wavelength (488 nm).

$$\left\langle \phi_f \middle| \phi(t)\right\rangle = \prod_k \left\{ \exp\left[-\frac{\Delta_k^2}{2}\left(1-\exp\left(-i\omega_k t\right)\right) - \frac{i\omega_k t}{2}\right] \times \left(1-\exp\left(-i\omega_k t\right)\right)^{n_k} \times \frac{\left(-1\right)^{n_k}\Delta_k^{n_k}}{\left(2^{n_k} n_k!\right)^{1/2}} \right\} \quad (3)$$

ure 4. Identical total distortions are obtained for both complexes, further corroborating the consistency of our analysis. The luminescence and absorption spectra for both complexes studied here can be calculated from the parameters in Table 1 and are shown for comparison in Figure 3 and Figure 4. These spectra are calculated without any adjustable parameters and the good agreement further illustrates that the parameters in Table 1 are physically meaningful.

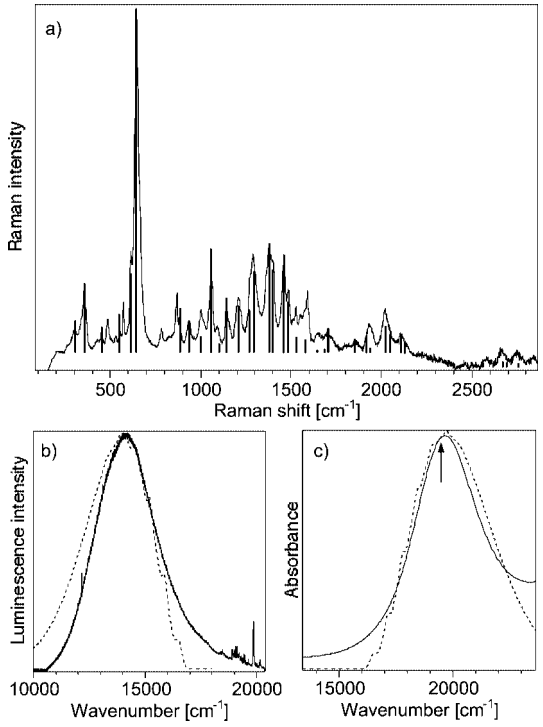

Figure 4. Comparison of calculated and experimental spectra for [Ru(BQDI)(acac)$_2$]. a) Resonance Raman, b) 77 K solid-state luminescence and c) room-temperature absorption in dimethylformamide solution. The calculated spectra in b) and c) are given as dotted lines. The vertical arrow in c) denotes the resonance Raman excitation wavelength (514 nm).

The calculations show that the largest excited state distortion occurs along the coordinate associated to the mode with a frequency of approximately 650 cm^{-1}, in agreement with the qualitative observation made before, and distortions of identical magnitude are obtained for both complexes. The quantitative analysis allows more general observations to be made. We can separate the excited-state distortions into two groups, one containing modes whose frequencies are between 300 and 650 cm^{-1} and whose displacements are relatively high, and another group containing modes with higher frequencies between 1000 and 1500 cm^{-1} and lower displacements. The latter group can be assigned to ligand-centered modes, whereas the former is clearly related to metal-ligand modes. This observation is in agreement with the proposed MLCT character of the transition, and shows that both complexes are quite similar, despite the minor differences discussed previously. This suggests that the BQDI ligand plays a major role in the electronic transition, as acceptor of charge, and that the auxiliary ligands modify the electronic structure of the entire complex in a slightly different manner for the two complexes studied here, as shown by the resonance Raman intensities and the analysis based on time-dependent theory. Much larger effects of auxiliary ligands on a variety of chemical properties of this category of complexes are discussed elsewhere.[18] However, it is critical to note that the primary changes in geometry in the excited MLCT states occur within the Ru–N^{a}H=C–C=N^{b}H(*Ru–N^b*) metallacycle, which is quasi aromatic (6-electron ring) with much less distortion within the six membered benzene ring of BQDI. Indeed one might describe the transitions as mainly π–π* within the quasi aromatic metallocycle ring system. Our results show that the excited-state distortions in the title complexes can be explored by resonance Raman spectroscopy in unprecedented detail not accessible for other charge-transfer excited states in ruthenium(II) complexes.

Experimental Section

The species [Ru(BQDI)(NH$_3$)$_2$Cl$_2$] and [Ru(BQDI)(acac)$_2$] were prepared by literature methods.[18,23] Raman spectra were measured with a Renishaw 3000 Raman imaging microscope at 488, 514 and 788 nm excitation laser wavelengths. The microscope was used to focus the light onto a spot of approximately 1 μm in diameter and to collect the scattered light. The backscattered Raman light was detected with a Peltier cooled CCD detector. This instrument was also used to measure luminescence spectra. Absorption spectra were measured with a Varian Cary 5E spectrometer.

Density functional theory (DFT) spin-restricted calculations were performed using the Gaussian 03 program (Revision C.01 and C.02).[24] Optimized geometries were calculated by using the B3LYP exchange-correlation functional[25,26] with the LanL2DZ basis set.[27–30] The SWIZARD program[31] was used to extract the calculated Raman spectra from the Gaussian output files with a line width of 15 cm^{-1}.

Acknowledgments

We thank the Natural Sciences and Engineering Research Council of Canada for financial support and Harini Kaluarachchi and Daria Kalinina for laboratory assistance.

[1] J. I. Zink, *Coord. Chem. Rev.* **2001**, *211*, 69.
[2] J. L. Wootton, J. I. Zink, *J. Am. Chem. Soc.* **1997**, *119*, 1895.
[3] K.-S. K. Shin, J. I. Zink, *J. Am. Chem. Soc.* **1990**, *112*, 7148.
[4] K.-S. K. Shin, J. I. Zink, *Inorg. Chem.* **1989**, *28*, 4358.
[5] L. Tutt, J. I. Zink, *J. Am. Chem. Soc.* **1986**, *108*, 5830.
[6] Y.-J. Chen, P. Xie, J. F. Endicott, O. S. Odongo, *J. Phys. Chem. A* **2006**, *110*, 7970.
[7] J. T. Hupp, R. D. Williams, *Acc. Chem. Res.* **2001**, *34*, 808.
[8] G. D. Danzer, J. R. Kincaid, *J. Raman Spectrosc.* **1992**, *23*, 681.
[9] S. K. Doorn, J. T. Hupp, *J. Am. Chem. Soc.* **1989**, *111*, 4704.
[10] L. C. T. Shoute, G. R. Loppnow, *J. Am. Chem. Soc.* **2003**, *125*, 15636.
[11] J. Streiff, J. L. McHale, *J. Chem. Phys.* **2000**, *112*, 841.
[12] C. J. Da Cunha, S. S. Fielder, D. V. Stynes, H. Masui, P. R. Auburn, A. B. P. Lever, *Inorg. Chim. Acta* **1996**, *242*, 293.
[13] S. I. Gorelsky, E. S. Dodsworth, A. B. P. Lever, A. A. Vlcek, *Coord. Chem. Rev.* **1998**, *174*, 469.
[14] A. B. P. Lever, S. I. Gorelsky, *Coord. Chem. Rev.* **2000**, *208*, 153.
[15] H. Masui, A. B. P. Lever, E. S. Dodsworth, *Inorg. Chem.* **1993**, *32*, 258.

[16] R. A. Metcalfe, E. S. Dodsworth, S. S. Fielder, D. J. Stufkens, A. B. P. Lever, W. J. Pietro, *Inorg. Chem.* **1996**, *35*, 7741.
[17] R. A. Metcalfe, A. B. P. Lever, *Inorg. Chem.* **1997**, *36*, 4762.
[18] J. Rusanova, E. Rusanov, S. I. Gorelsky, D. Christendat, R. Popescu, A. A. Farah, R. Beaulac, C. Reber, A. B. P. Lever, *Inorg. Chem.* **2006**, *45*, 6246.
[19] E. I. Solomon, *Inorg. Chem.* **2006**, *45*, 8012.
[20] E. J. Heller, *Acc. Chem. Res.* **1981**, *14*, 368.
[21] E. J. Heller, R. L. Sundberg, D. Tannor, *J. Phys. Chem.* **1982**, *86*, 1822.
[22] S.-Y. Lee, E. J. Heller, *J. Chem. Phys.* **1979**, *71*, 4777.
[23] K. N. Mitra, S. Choudhury, A. Castińeiras, S. Goswami, *J. Chem. Soc., Dalton Trans.* **1998**, 2901.
[24] M. J. Frisch, G. W. Trucks, H. B. Schlegel, G. E. Scuseria, M. A. Robb, J. R. Cheeseman, J. J. A. Montgomery, T. Vreven, K. N. Kudin, J. C. Burant, J. M. Millam, S. S. Iyengar, J. Tomasi, V. Barone, B. Mennucci, M. Cossi, G. Scalmani, N. Rega, G. A. Petersson, H. Nakatsuji, M. Hada, M. Ehara, K. Toyota, R. Fukuda, J. Hasegawa, M. Ishida, T. Nakajima, Y. Honda, O. Kitao, H. Nakai, M. Klene, X. Li, J. E. Knox, H. P. Hratchian, J. B. Cross, V. Bakken, C. Adamo, J. Jaramillo, R. Gomperts, R. E. Stratmann, O. Yazyev, A. J. Austin, R. Cammi, C. Pomelli, J. W. Ochterski, P. Y. Ayala, K. Morokuma, G. A. Voth, P. Salvador, J. J. Dannenberg, V. G. Zakrzewski, S. Dapprich, A. D. Daniels, M. C. Strain, O. Farkas, D. K. Malick, A. D. Rabuck, K. Raghavachari, J. B. Foresman, J. V. Ortiz, Q. Cui, A. G. Baboul, S. Clifford, J. Cioslowski, B. B. Stefanov, G. Liu, A. Liashenko, P. Piskorz, I. Komaromi, R. L. Martin, D. J. Fox, T. Keith, M. A. Al-Laham, C. Y. Peng, A. Nanayakkara, M. Challacombe, P. M. W. Gill, B. Johnson, W. Chen, M. W. Wong, C. Gonzalez J. A. Pople, in Gaussian 03, C02., Gaussian, Inc., **2004**.
[25] A. D. Becke, *J. Chem. Phys.* **1993**, *98*, 5648.
[26] C. Lee, W. Yang, R. G. Parr, *Phys. Rev. B* **1988**, *37*, 785.
[27] J. T. H. Dunning, P. J. Hay, in *Modern Theoretical Chemistry*, vol. 3 (Ed.: I. H. F. Schaefer), Plenum, New York, **1976**, p. 1.
[28] P. J. Hay, W. R. Wadt, *J. Chem. Phys.* **1985**, *82*, 270.
[29] P. J. Hay, W. R. Wadt, *J. Chem. Phys.* **1985**, *82*, 284.
[30] P. J. Hay, W. R. Wadt, *J. Chem. Phys.* **1985**, *82*, 299.
[31] S. I. Gorelsky, SWizard program, revision 4.2, http://www.sgchem.net/swizard/.

Received: October 1, 2006
Published Online: November 17, 2006

